

HEAT TRANSFER AND CARRYOVER IN THE DRYOUT OF A HEATED VERTICAL TUBE

A. Heydari

Department of Mechanical Engineering
Sharif University of Technology
Tehran, Iran

Abstract This work concerns dryout experiments in which a tube, initially containing water, filled up or partially filled and at 1, 2 or 3 atmosphere pressures, is heated. The initial water column experience three thermal regions. The first region, called the first period, involves heating of the tube until saturation conditions are obtained in the water. Boiling of the water in the tube causes swelling with overflow at the top of the tube, which happens during the second period. The second period ends when the overflow ceases. Hereafter, the liquid content of the tube diminishes because of evaporation, its level falls and exposes the tube wall to vapor, and the temperature of the exposed tube rises. This occurrence is called dryout; the period in which it occurs is called the third period. The experimental results of 44 dryout experiments are the histories of dry-out level collapsed liquid level, and tube wall temperatures. The analytical objective is the prediction of the temperature, collapsed liquid level and the dryout histories during the three periods. The temperature history of the first period is predicted according to a result of Jaeger [4]. The collapsed liquid level, quench front and the transient height of the two-phase level during the second period are predicted by a model developed by Lahey [6]. Once dryout begins, a drift flux model by Sun et al [10] predicts the history of the dry-out and the collapsed liquid level. The wall temperature above the dryout level is predicted using a model by Yeh et al. [5]. Good agreements between the experimental results and the predictions were found for the first and third periods but the duration of the second period could not be correctly predicted.

Key Words Two-Phase Flow, Heat Transfer, Dryout, LOCA, PWR, Carryover, Vertical Tube, Loss of Coolant, Thermohydraulics, Reactor Safety.

چکیده مقاله حاضر مسئله خشک شدن در یک لوله عمودی حرارت داده شده که در ابتدا حاوی آب می باشد را بطور تجربی و عددی مورد بررسی قرار می دهد. ملاحظات آزمایشگاهی در سه فاصله زمانی مورد بررسی قرار گرفته و در هر پریود با نتایج مدل‌های عددی مقایسه شده است. مدل‌های ریاضی و روابط تجربی مقادیر دما، سطح مایع فرو ریخته و تاریخچه خشک شدن در هر سه پریود را پیش بینی می کنند. در بررسی تاریخچه دما در پریود نخست از نتایج مأخذ ۴ استفاده شده است. سطح مایع فرو ریخته در پریود دوم از تجزیه و تحلیل مأخذ ۶ بدست آمده است. دمای دیواره در بالای سطح مایع نیز بوسیله مدل مأخذ ۵ پیش بینی شده است. بین نتایج عددی پریود اول و سوم و ملاحظات آزمایشگاهی توافق خوبی وجود دارد ولی مدل ارائه شده برای محاسبه زمان پریود دوم نتایج مناسبی را ارائه نمی دهد.

INTRODUCTION

A process of great significance with impact on obtaining a license for a Light Water Reactor (LWR) is the re-cooling of the core after a hypothetical Loss-Of-Coolant-Accident (LOCA) has occurred. The drying out of a reactor core by the boiling-off of the coolant inventory, due to a continued heat input to the water is known as a dryout event. Accidents

such as Three Mile Island and Chernobyl indicate the importance of the ability to predict the dryout history, the water inventory level and the thermal-hydraulic behavior above the two-phase level during the dryout conditions. Subsequent analysis of accidents has shown the need for both experimental results pertinent to the dryout values as well as development of models to describe the thermal-hydraulic behavior of coolant within the reactor core

during a dryout event.

In this work we develop analytical models and compare the prediction of the models to the experiment results of 44 tests performed using a reflood-dryout facility which consisted of a 12.5ft (3.81m) high Inconel tube with an inside diameter of 0.56 in (14.22mm).

A test was initiated by initializing experimental and recording instrumentation, introducing water into the test tube to 12.5 ft (3.81m), 6.5 ft (1.98 m) or 4 ft (1.22m) level, pressurizing the test section (only for non-atmospheric runs), heating the metering system as well as the collector and the separator assembly and then heating the tube and the stagnant water system by applying power to the tube. The captured water reaches saturation conditions from a supposedly initial equilibrium condition. The period in which water temperature reaches the saturation throughout the tube is referred to as the first period. Soon after, exists a period of sudden boil-off or swelling of the water inventory, here called the second period. The water inventory in the test tube is sealed below and open above, causing depletion of the water level and the formation of a liquid film on the interior area of the tube.

After a sufficient time and starting from the top of the tube the two phase mixture is vaporized causing dryout in the highest location of the test tube. A dryout front gradually descends and evaporates liquid over the surface of the gradually decreasing liquid level. this period which starts from the end of the second period and involves evaporation of the liquid film left on the tube surface after the boil-off period and the drying-out of the test tube is called the third period.

Figure 1 shows a schematic representation of the uniformly-heated vertical tube and the associated flow patterns along the tube. Under the two-phase level, three flow regimes of annular, churn-turbulent, and slug flow are identified, while above the dryout level, the flow regime is generally dispersed droplet flow or single-phase steam.

This report presents the experimental results with an analysis and modeling of the boil-off and dryout process in the context of the three designated periods. The predicted

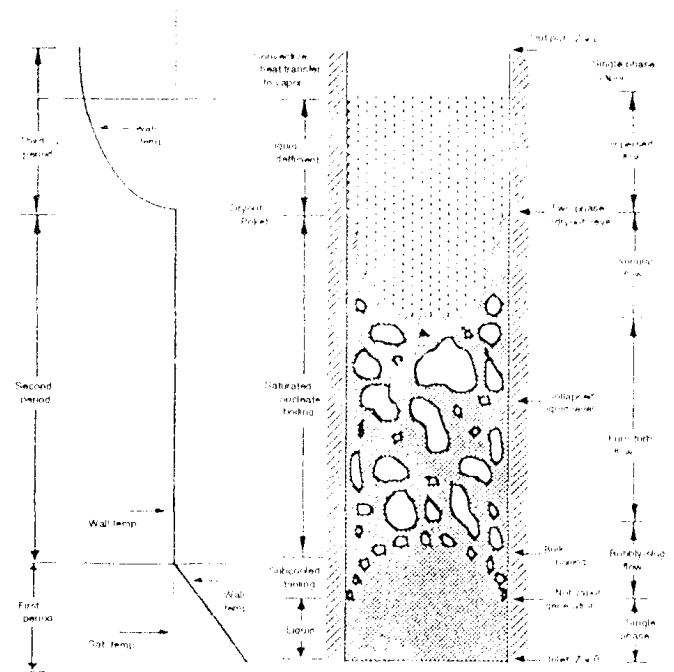


Figure 1. Flow regime of a uniformly heated vertical tube

values include the temperature history of different recording levels, dryout history of the third period, instantaneous height of the swelling column (for partially-filled runs), and the history of collapsed liquid level, abbreviated as C.L.L., (a measure of the water level in the absence of vapor voids) inside of the tube.

EXPERIMENTAL RESULTS

Experimental Set Up

The experimental system is shown schematically in Figure 2. Physical specifications of the tube are shown in Table 1. A major component of the experimental system is an inconel test tube of 12.5 ft height. The system also consists of a separator used for separating liquid and vapor phases leaving the tube which is mounted above the test tube, a collector used for collecting the liquid phase from the separator, and a steam meter in which the steam flow rate from the separator was determined by pressure drop through the steam venturi. Water was supplied to the bottom of the tube from the feedwater supply system and tank. Eleven type K chromel-alumel thermocouples, of 30 gauge, were

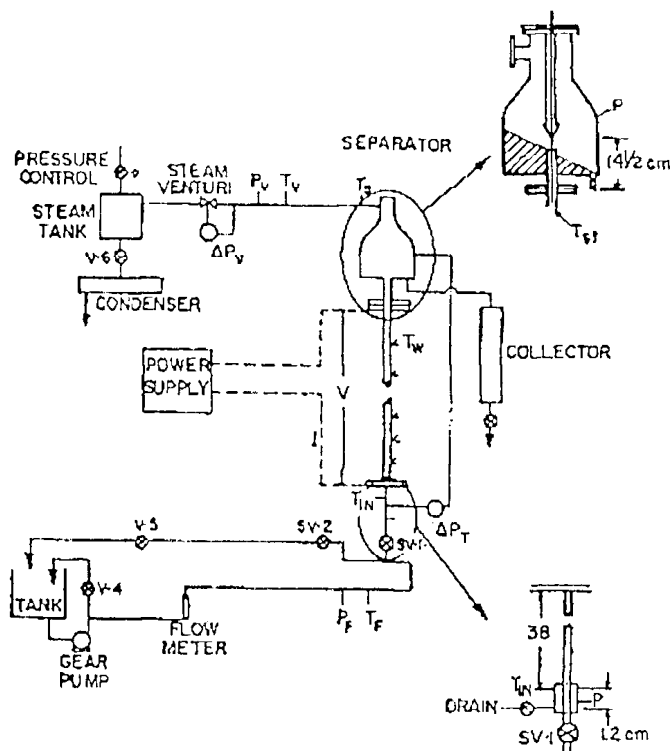


Figure 2. Schematic of the experimental system.

spot welded to the outside of the test tube at one ft intervals. A power supply provided direct current to the tube wall, through connections made at the top and bottom flanges of the tube.

A more detailed description of the experimental set-up and each component is reported by R.A.Zogg [2]. Step by step test procedures taken in the process of making experimental runs are outlined by T. La Jeunesse [3].

A test was initiated by pumping distilled water from the feedwater supply system into the tube to a level of 12.5 ft, 6.5 ft or 4 ft depending on the particular test conditions. The inlet valve was closed and a given power level was applied to the test section. Recording devices such as a strip chart recorder and an Autodata data collector were turned on after 10-15 seconds.

Once the desired input power and system pressure were set, the data acquisition system recorded the temperature history of the thermocouples, the input power, the system pressure, the venturi readings, pressure difference in the collector and across the test tube. The test ended after dryout was observed at the one ft level.

TABLE 1. Test Tube Specifications

Length	12.5 ft (3.81 m)
Inside Diameter	0.56 in (14.22 mm)
Outside Diameter	0.626 in (15.9 mm)
Wall Thickness	0.0325 in (0.83 mm)
Thermal Conductivity	9 Btu/(hr-ft-F) (15.6 W/m-C)
Density	525 lbm/ft ³ (8410 Kg/m ³)
Specific Heat	$= 0.1046 + 0.0276(T + 0.5 \times 10^{-9})T^2$ Btu/lb-F
Resistance per unit length	for $70 \text{ F} < T < 1000 \text{ F}$ ohms/ft for $T > 1000 \text{ F}$ $R = 8.91 \times 10^{-3}$ ohms/ft

Experimental Results

Altogether 44 tests were taken, out of which 27 were for completely-filled runs and the rest for partially-filled runs. Furthermore, these tests were obtained at system pressures of 1, 2, and 3 atmospheres. For each system pressure a range of input powers, from approximately 500W-7000W, was examined with, in most cases, at least one repeated run for each test condition. This was done in order to confirm the test results.

In this section two typical results, one for an initially full tube and the other for a partially full tube, are presented. Complete Tables of the experimental data are given in Reference 1.

A Typical Run with an Initial Fill Height of 12.5 ft

Run 3153B taken for a pressure of 1 atm, is shown here as typical of runs with an initial fill height of 12.5 ft. An input power of 2532 watts was applied to the test tube after water was pumped into the test section and after the system components achieved desired temperatures. Figure 3 shows wall temperature histories for all connected thermocouples. The wall temperatures rise almost linearly to about 212 F, the saturation temperature, and thus the time for the saturation of the 11 positions is in the range of 0.87 - 1.15 minutes.

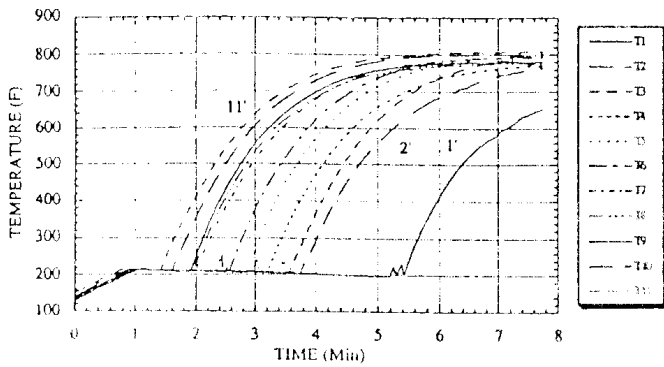


Figure 3. Tube wall temperature history of run #3153B

Figure 4 shows the history of the actual liquid mass inside the tube, evaluated as the collapsed liquid level. In most runs saturation temperature is attained at different times for different elevations, as in this run, and so in order to express the time the entire tube attains saturation, there is used t_l (see Figure 4), when there is a sharp drop in the history of the liquid content of the tube. This time is found from Figure 4 to be $t_l = 0.85$ minutes. The time t_l marks the time when the first period ends and the second period starts. After the onset of boiling ($t_l = 0.85$ min), there is a period of rapid generation of voids in the tube, so that a substantial part of the initial water inventory is forced out of the test tube into the collector because of the bulk boiling of the water inside the tube. This rapid decrease of the collapsed liquid level is known as pool swelling. The end of the second period and the start of third period, at time t_k (see Figure 4), is defined to occur when the rapid drop of the collapsed liquid level ceases and there exists a visible and definable change in the slope of the collapsed liquid level history. For run # 3153B this happens at time $t_k = 1.25$ minutes. During the second period the wall temperature remains almost constant until dryout happens at the top of the test tube (12.5 ft location). Dryout at a recording location is defined to occur when the wall temperature rises sharply from a prior constant value. As boiling begins at various locations inside the tube during the first period, the swollen liquid level rises to the top of the tube during the second period, with subsequent overflow and stays there until the end of the overflow. Subsequent heating

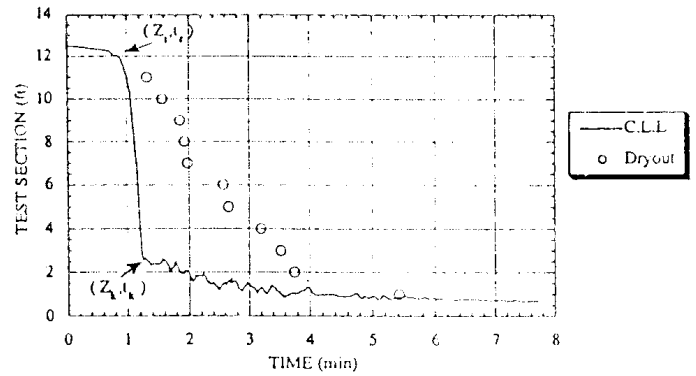


Figure 4. Dryout and collapsed liquid level of run #3153B

causes evaporation of water inside the tube in the form of a dry-out front moving from top towards the bottom of the tube. Note that the first recorded dryout location is at the eleven-ft level and subsequent dryout is observed at one-ft level under the 11 ft location. Figure 4 shows dry-out and collapsed liquid level heights, called Z_l & Z_k respectively, as a function of time. The dryout level decreases somewhat irregularly.

The phases of the water leaving the test section are separated, with the liquid passing, by gravity, into the collector tank and the vapor through a superheater to the venturi meters. Figure 5 shows the mass accumulated in the collector and the total vapor produced, evaluated as an integral of the mass flow rate indicated by the venturi meter pressure output. The sum of test section, collector and the steam mass forms the total mass, which shows 20% (0.23 lbm) loss during the experiment.

A Typical Run with an Initial Fill Height of 6.5 ft

Run 3157A is taken as typical partially-filled runs with the tube filled to half of its height and with an input power of 2450 Watts. The fill level was chosen so as to leave enough space above the initial water height for examining the rate and height of the expanding water level.

Figure 5 is the temperature history for run 3157 A. As with most partially-filled runs this typical run shows an initial non-uniform wall temperature. The initial wall temperature of levels below 6.5-ft level is between 140 -

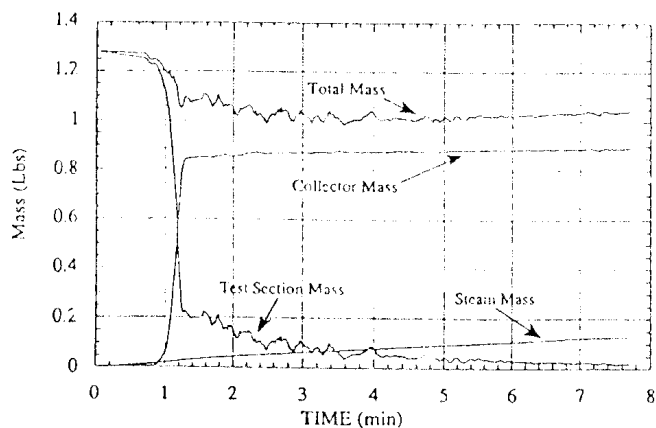


Figure 5. System mass history of run #3153B

190 F. Temperatures of levels above the initial fill rise more rapidly with time than do those below: at 6 ft (0.5 ft below fill level) temperature is somewhat higher compared to locations below, and at 7 ft (0.5 ft above fill level), temperature lower than they are above. This is consistent with trend expected from wall heat conduction with higher temperatures existing above the fill level. Temperature histories are similar to those of the initially filled runs except for during the first 0.75 minutes for locations above the initial fill level (i.e. above 6.5 ft for this run). Once saturation temperature is reached bulk swell of the water inventory wets and quenches elevations above the initial fill level, causing their temperatures to drop to the saturation level. The temperature profile during the third period is similar in nature to that of the initially-filled runs.

Figure 7 shows the dryout histories as well as the collapsed liquid level for 3157 A. The features are similar

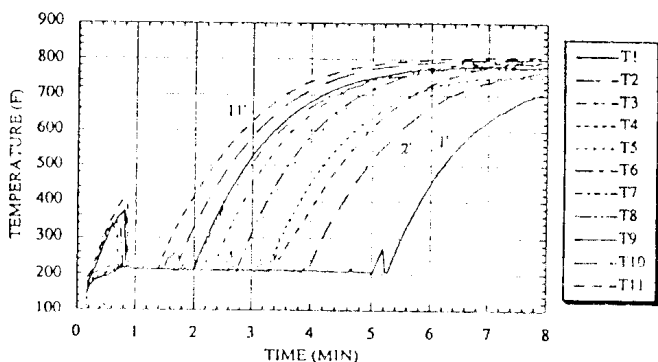


Figure 6. Tube wall temperature history of run #3157A

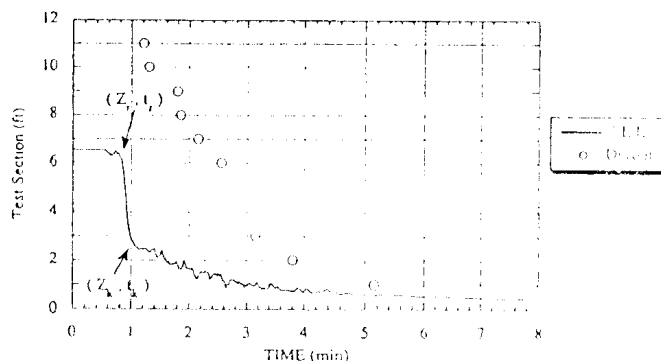


Figure 7. Dryout history and collapsed liquid level of run #3157A

to those of Figure 4 of the full tube. The duration of the first period is taken from Figure 7 to be $t_f = 0.65$ min and the end of second period happens at time $t_k = 0.95$ min. Figure 8 exhibits the history of the overall mass of the fluid in the experimental system, the mass as a function of time in the test section, the collector and the steam mass passing through the venturi. Again the total mass history indicates 0.48 lbm of the initial fill leaves the test assembly.

ANALYSIS AND PREDICTIONS OF THE FIRST PERIOD

First Period

A test began with the input of power to the test tube,

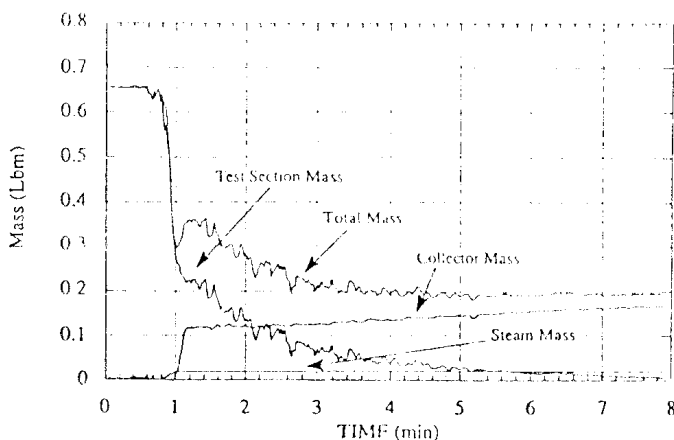


Figure 8. System mass history of run #3157A

followed by the start of the tape record. Initially there is an almost linear increase in wall temperature for the region in which water is contained in the tube and a more rapid and non linear rise above this level for the partially-filled tube. There the tube interior contains air. The first period ends when the tube wall temperature attains the saturation value (see Figures 3 or 6), which is near or at the time when the mass contained in the tube begins to decrease rapidly and the mass in the collector begins to increase (Figures 5 and 8). Because of different wall temperature behaviors for the filled-up and the partially-filled runs, these two situations are considered and analyzed separately.

Filled-Up Runs

The heat transfer during the first period for the filled-up runs takes place between a heated tube internally in contact with a column of water at an initial wall temperature, T_i , ideally constant and uniform throughout the tube.

The thermal properties of the tube differ from those of the water. Because the tube wall is relatively thin and its thermal conductivity much greater than that of the water, the radial variation of temperature in the tube can be assumed constant as a first approximation. Even this does not simplify substantially the heat conduction problem and as an approximation there is predicted the temperature history from the conduction solution for a cylinder of water, with the thermal capacity of the tube and heat loss to the ambient considered as a boundary condition. The solution is [4]:

$$\frac{\Delta T K_f}{q D} = \frac{K_f}{h_L D} - \sum_{n=1}^{\infty} \frac{e^{-\alpha_f \kappa_n^2 t} J_0(r \kappa_n)}{\left\{ \left[1 + \frac{2 \delta C_{p,w} \rho_w}{a C_{p,f} \rho_f} \right] (a \kappa_n)^2 + \frac{1}{4} \left[\frac{h_L D}{K_f} - \frac{2 C_{p,w} \rho_w a \delta \kappa_n^2}{C_{p,f} \rho_f} \right]^2 \right\} J_0(a \kappa_n)} \quad (1)$$

where;

$\Delta T = T_r - T_i$ = Difference of the temperature of radial

location r and the initial water temperature

h_L = Heat transfer coefficient between tube wall and the ambient; (Btu/(hr - ft²-F))

$$h_L = 2.37 e^{(1.44 \times 10^{-3}(T_w - T_\infty))} \quad (2)$$

α_f = Thermal diffusivity of the water; (ft²/hr)

κ_n , $n = 1, 2, 3, \dots$ are the positive roots of the equation:

$$\left(\frac{h_L a}{K_f} - \frac{\delta C_{p,w} \rho_w}{a C_{p,f} \rho_f} (a \kappa_n)^2 \right) J_n(a \kappa_n) - a \kappa_n J_n'(a \kappa_n) = 0 \quad (3)$$

Reference 1 shows the results of using Equation 1 for obtaining t_{sat} of the initially-filled runs, for different initial water temperatures. The model predicts an almost linear temperature rise from the initial wall temperature to the saturation temperature, which agrees with the experimental data. The calculated duration of the first period depends on the initial wall temperature, but based on the slopes of the calculated and experimental histories, there exists a fair comparison between the predicted and experimental results.

Partially-Filled Runs

The temperature behavior of levels below the initial fill level is similar to that of the initially-filled runs.

The heat transfer model to predict the wall temperature history of partially-filled runs for over-the-initial water level during the first period, which is an extension of that developed by Yeh, Chiou and Young [5] is based on the assumption that the temperature of tube is radially uniform and the axial conduction is negligible. With these, the thermal behavior for levels above the liquid level is given by:

$$P - h_L A_f (T_w - T_\infty) = M_w C_{p,w} \frac{dT_w}{dt} \quad (4)$$

here h_L is the heat transfer coefficient for the tube heat loss

to the ambient, given by Equation 2. Since h_l depends on T_w , Equation 4 is solved numerically for the wall temperature.

The predictions for the under-the-fill levels of the partially-filled test give the same conclusions as for the initially-filled runs. There is also predicted the temperature profile of the elevations above the fill level for the partially-filled runs. Based on the comparisons made between the calculated values of T_w and the experimental results, Reference 1 shows that for most runs there is a fair agreement between the results of the thermal model and the experimental results.

ANALYSIS AND PREDICTIONS FOR THE SECOND PERIOD

Second Period

The second period is defined to begin at the time when the entire water-filled portion of the tube reaches bulk saturation. There exists a period of rapid swelling soon after the water column content of the tube attains boiling. The swelling of water is experimentally indicated by a sudden drop in the collapsed liquid level from its initial height of Z_r at time t_r . The second period which lasts only for seconds and during which water is discharged out of the test tube into the collector, ends at time t_k with a collapsed liquid level height of Z_k (see Figure 4). For the partially-filled runs, the swelling of the fluid contained in the tube wets the tube surface at level over that of the initial fill, causing the high temperatures existing there to drop to saturation temperature.

Here we formulate the void fraction as a function of tube height as well as time for the second period. Of particular interest is calculation of the history of the collapsed liquid level, the height of the rising pool surface, the duration of the second period, and the temperature history of levels above the fill for the case of partially filled runs. The analysis presented here was originally due to Lahey [6] and Epstein [7]. This report utilizes the model of

Lahey and includes in it the variation of the void distribution parameter, C_o .

Pool Swell Model

A liquid pool of initial height H_o is contained in a vertical tube. Initially, the liquid is at saturation temperature and boiling begins at zero time. The analysis is based on the Zuber [8] model for two phase flow, which incorporates two parameters C_o and V_{gj} , C_o to correct for the radial variation of the void fraction and V_{gj} to express the difference between the gas velocity and the mass velocity for the two phase mixture.

For a two-phase system in vertical motion, a common expression for the drift velocity is of the form

$$V_{gj} = V_{\infty} (1 - \alpha)^n \quad (5)$$

where V_{∞} is the terminal rise velocity of bubbles in a stagnant pool [9]. The exponent n depends on the viscosities of the two phases and on the type of the flow regimes. An appropriate value of V_{∞} and index n is determined from the analysis of experimental results.

The Void Distribution Equation

Combining the continuity equation for one-dimensional two-phase flow in a tube of constant cross-sectional area gives the one-dimensional void propagation equation as:

$$\frac{d\alpha}{d\theta} + (C_o J + \alpha \frac{dV_{gj}}{d\alpha} + V_{gj}) \frac{d\alpha}{dz} = \frac{\Gamma}{\rho_g} (1 - C_o \alpha) \quad (6)$$

where Γ is the void generation term, which for an isothermal system in thermodynamic equilibrium and at constant pressure is given as:

$$\Gamma = \frac{Q'}{h_{fg} A_c} \quad (7)$$

for $B = \frac{Q' v_{fg}}{A_c h_{fg}}$ Equation 7 becomes $\Gamma = \frac{B}{v_{fg}}$ (8)

In deriving Equation 7, in addition to the above assumptions, the instantaneous energy released due to quenching of the heated tube by the rising swollen liquid level at the quench location is also neglected. Consideration of these effects requires solving the momentum equation, which further complicates the solution and has not been considered.

Solution of the Void Propagation Equation

The solution of the integral surface $\alpha = \alpha(z, \theta)$ Equation 6 is equivalent to the solution of the following set of ordinary differential equations:

$$d\theta = \frac{dz}{\left[C_0 J + \alpha \frac{dV_{g1}}{d\alpha} + V_g \right]} = \frac{d\alpha}{\frac{\Gamma}{\rho_g} (1 - C_0 \alpha)} \quad (9)$$

Integrating the first and the third ($\theta - \alpha$) ordinary differential equation and also second and the third ($z - \alpha$) differential equations and applying boundary conditions of $\alpha=0, \theta=0, z=0$ gives us the following characteristics:

$$\alpha = \frac{1 - e^{-C_0 B \theta}}{C_0} \quad (10)$$

$$z = \frac{V_{\infty} \alpha (1 - \alpha)^n}{B(1 - C_0 \alpha)} \quad (11)$$

Equation 11 which gives the characteristic emanating from the initial condition of $\alpha=0, z=0, \theta=0$ is called the limiting characteristic, Z_w , given by:

$$Z_w = \frac{V_{\infty} (1 - e^{-BC_0 \theta})}{C_0 B e^{-BC_0 \theta}} \left(\frac{C_0 - 1 + e^{-BC_0 \theta}}{C_0} \right)^n \quad (12)$$

where θ is time difference with reference to the beginning of the second period, i.e. $\theta = t - t_1$.

The swell analysis of the second period is divided into two regions. Region 1 which is above the limiting characteristic (i.e. $Z_w < z < H_1$) is characterized by a constant void fraction and is called the transient boiling region. Region 2 is steady-state boiling and is below the limiting characteristic (i.e. $0 < z < Z_w$) with a void fraction less than that of the first region.

For transient boiling region, $z > Z_w$, the void fraction is a function of θ alone and is given by Equation 10. For the steady boiling region, $z < Z_w$, the void fraction is a function of z alone and is given by Equation 11.

Pool-Swell Height for Partially-Filled Runs

The transient height, $H(\theta)$, of the swelling pool propagating upward in the tube, marks the z location where the transient boiling region is abruptly terminated and the void fraction equals 1.

The swell (or quench) level $H(\theta)$ is found from a balance of the total liquid content of the tube to be:

$$H(\theta) = \frac{H_c + \frac{\Delta p}{\rho_f} \left[\int_0^{z_w} \alpha dz - \alpha_w Z_w \right]}{\left(1 - \frac{\Delta p}{\rho_f} \alpha_w \right)} \quad (13)$$

In deriving Equation 13 it is assumed that no liquid leaves the quench level. Equation 13 is solved numerically. The next two sections use the solution for $H(\theta)$ to calculate duration of pool-swelling and the collapsed liquid level history, during the second period.

Duration of the Second Period

The experimental results shows the swelling period ceases (indicated by flattening of the collapsed liquid level history) at the same time the water carry-over into the separator

ends. In terms of the second period analysis the end of the second period happens when there is no longer a transient region, or when the limiting characteristic reaches the height of the two-phase level, i.e. $Z_w(\theta_k) = H(\theta_k)$. Using Equation 12 and 13 the duration of the second period is found from the following equation;

$$Z_w(\theta_k) = \frac{H_0 + \frac{\Delta\rho}{\rho_l} \left[\int_0^{z_w(\theta_k)} \alpha dz - \alpha_w(\theta_k) Z_w(\theta_k) \right]}{\left(1 - \frac{\Delta\rho}{\rho_l} \alpha_w(\theta_k) \right)} \quad (14)$$

Collapsed liquid level

Another value of interest is the collapsed liquid level, Z_c , defined as;

$$Z_c(\theta) = \int_0^{H(\theta)} (1 - \alpha) dz \quad (15)$$

Dividing the integral into two parts, we have;

$$Z_c(\theta) = \int_0^{Z_w(\theta)} (1 - \alpha) dz + \int_{Z_w(\theta)}^{H(\theta)} (1 - \alpha) dz \quad (16)$$

but with $\alpha = \alpha_w(\theta)$ for $z \geq Z_w(\theta)$;

$$Z_c(\theta) = H(\theta)(1 - \alpha_w(\theta)) + \alpha_w(\theta) Z_w(\theta) - \int_0^{z_w(\theta)} \alpha dz \quad (17)$$

Equations 13, 14 and 15 are solved numerically. Reference 1 shows analytical solution of these equations for the cases of $n = 0$ and $n = 1$.

The calculations indicate that the model fails to predict a reasonable time for the duration of the second period. That causes the predicted collapsed liquid level to drop much faster than the experimentally observed histories, while there is a fair similarity between the final value of the collapsed liquid level obtained numerically and those observed experimentally. The temperature history of above the fill elevations of the partially-filled runs is the

continuation of the temperature history predicted during the first period until the swelling height wets the tube. The calculated duration of the second period is so short that the wall temperature of over-the-fill elevations of partially-filled runs drop instantly from their values at the end of the first period to the saturation level.

ANALYSIS AND PREDICTIONS FOR THE THIRD PERIOD

Third Period

The third period is defined to begin at the end of the second period, at time t_k . The experimental results indicate that the process of the dryout starts from the highest elevation and a dryout front gradually moves downward causing dryout of the entire test tube. The phenomenon is similar for both filled-up and partially-filled runs.

Dry-Out Model

It is assumed that if the transient two-phase level behavior is sufficiently slow, a quasi-steady analysis is appropriate for the third period. With this the temporal changes are assumed to be small compared to the spatial variations. The transient two-phase flow is also assumed to be in thermal equilibrium but not homogeneous.

The following model predicting the dryout history of a heated vertical tube is originally due to Sun *et al.* [10]. Under the two-phase level multiple flow regimes, each with a distinct set of flow regime parameters (C_o & V_{gl}) are assumed to exist. Reference 11 shows the history of the collapsed liquid level, for the case of two-flow regimes, to be;

$$Z_c = Z_D \left(1 - \frac{1}{C_{o,1}} \right) - Z_T \left(\frac{1}{C_{o,0}} - \frac{1}{C_{o,1}} \right) + \left(\frac{V_{gl,0}}{C_{o,0}^2 B} \ln \frac{C_{o,0} B Z_T + V_{gl,0}}{V_{gl,0}} \right) + \frac{V_{gl,1}}{C_{o,1}^2 B} \ln \left(\frac{C_{o,1} B Z_D + V_{gl,1}}{C_{o,1} B Z_T + V_{gl,1}} \right) \quad (18)$$

where Z_D is the height of the two-phase level and Z_T is the transition height of the flow regimes in such a way that the flow regime parameters for $0 < z < Z_T$ are $C_{o,0}$ and $V_{gj,0}$ and for $Z_T < z < Z_D$ are $C_{o,1}$ and $V_{gj,1}$.

For only one flow regime in Z_c becomes;

$$Z_c = Z_D \left(1 - \frac{1}{C_{o,0}} \right) + \frac{V_{gj,0}}{C_{o,0}^2 B} \log \left(1 + \frac{B C_{o,0} Z_D}{V_{gj,0}} \right) \quad (19)$$

Assuming there is a negligible liquid carry-over during the third period, the history of the dry-out, $Z_{D,0}$, is shown in Reference 11 to be;

$$B_L C_{o,n}(t - t_{o,n}) = \log \left\{ \frac{C_{o,n} B Z_D + V_{gj,n} \left(\frac{Z_{D,0,n}}{Z_D} \right)^{C_{o,n}}}{C_{o,n}^2 B Z_{D,0,n} + V_{gj,n} \left(\frac{Z_{D,0,n}}{Z_D} \right)} \right\} \quad (20)$$

where:

$$B_L = \frac{\rho_g B}{\rho_L}$$

where $Z_{D,0,n}$ is the dryout level at time $t_{o,n}$, and index n takes values of 0 or 1. Should there exist more than one flow regime during the course of the dryout third period, flow regime dependent parameters of $C_{o,n}$ and $V_{gj,n}$ take the appropriate values of the regime existing in $Z_T < Z_D < H_L$, until, due to transition of one regime to another, $C_{o,n}$ and $V_{gj,n}$ change to reflect the characteristic of the other regime in $1 < Z_D < Z_T$. Also at the point of flow transition, the initial dryout height and time of the new flow regime (i.e. $Z_{D,0,n}$ and $t_{o,n}$) take last values calculated for the previous regime.

Heat Transfer above the Two-Phase Level

Heat transfer equations of the third period are similar to above-the-fill level equations of partially-filled runs of first and the second period. The only difference is that in the first and second period there is no significant gas flow above the liquid level and therefore heat transfer to the gas phase is negligible, while for the third period there is gas

produced by liquid evaporation.

Considering the transfer rate to the gas phase, the energy equations for the tube and the steam system becomes;

Energy balance of the tube:

$$M_w C_{p,w} \frac{dT_w}{dt} = P h_L A_w (T_w - T_\infty) - h_g A_w (T_w - T_g) \quad (21)$$

where h_g = heat transfer coefficient between tube and vapor interface, given below (Btu/h - ft² - F)

h_L = heat transfer coefficient between tube and the ambient, given by Equation 2 (Btu/h - ft² - F)

Also assuming quasi-steady steam flow, temporal changes of steam temperature are negligible, and so energy balance of the steam becomes:

$$\rho_g A_c B_g Z_D C_{p,g} \frac{dT_g}{dz} = h_g A_w (T_w - T_g) \quad (22)$$

In most cases the gas flow is turbulent and for it there is used the following equation (Dittus-Boelter) for the coefficient of heat transfer, h_g ;

$$\text{For } Re_D > 2200 ; Nu_D = 0.023 Re^{0.8} Pr^{0.4} \quad (23)$$

It is laminar only when Z_D is small or the heat flux input is very low. For laminar case we use the asymptotic value of $Nu = 4.364$, so;

$$\text{For } Re_D \leq 2200 ; Nu_D = 4.364 \quad (24)$$

where;

$$Re_D = \frac{4 m_g}{\pi \mu_g D} , M_g = \frac{\rho_g \pi D^2 B_g Z_D}{4} \text{ and } Nu_D = \frac{h_g D}{K_g} \quad (25)$$

Now using Equation 21 and 22 and formulating a finite difference scheme, we are able to predict the tube wall and steam temperature histories of the tube.

Using the experimental data for the first dryout time,

the predicted values of the dryout times of lower elevations, the histories of the collapsed liquid levels and the temperature profiles of different levels in the tube are obtained (see Reference 1). In all of our calculations the change in the flow regime inside the tube is considered by changing the values of the drift flux parameters C_o and V_{gj} . Three flow regimes are identified during the dryout as either Annular, Churn-turbulent, Slug, or a combination of the above. In general there exists a fair modeling of the dryout, collapsed liquid level and temperature history of both initially-filled and partially-filled runs. The breakdown of the dryout model occurs at lower power levels where the one-dimensional nature of the model may no longer be applicable.

COMPARISON TO THE EXPERIMENTAL RESULTS

Figures 9 and 10 present and compare the results of using the analytical temperature models developed for the three postulated periods. Figure 9 compares calculated and experimental temperature histories of three recording elevations of 11 ft, 6 ft and 1 ft for run #3153B. The predicted histories (dashed-lines) are close to the experimental values (solid lines). Similarly for the partially-filled runs, Figure 10 compares temperature histories of 11 ft, 3 ft and 1 ft levels for run # 3157A. Again dashed lines showing calculated values closely follow solid lines of the experimental data, indicating there exists a good agreement between the calculated and experimental results.

Figures 11 and 12 compare calculated collapsed liquid level and dryout histories for the initially-filled run # 3153B. Except for the much faster drop of the collapsed liquid level during the second period, there exists a good agreement between the calculated and the experimental values. Figures 13 and 14 and show a similar behavior for the typical partially-filled run # 3157A.

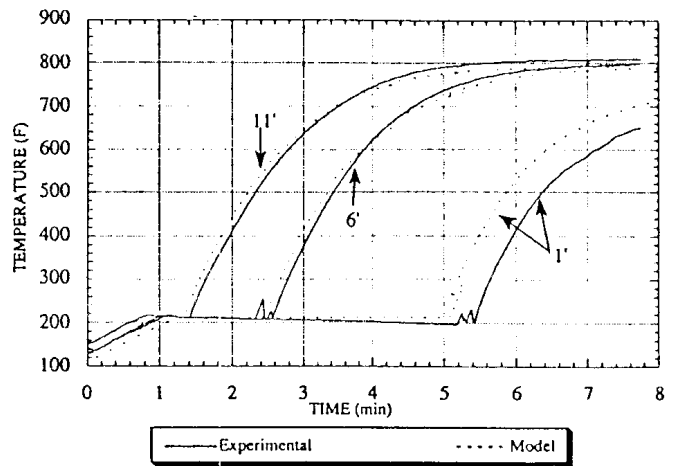


Figure 9. Comparison of calculated and experimental temperature histories for run #3153B

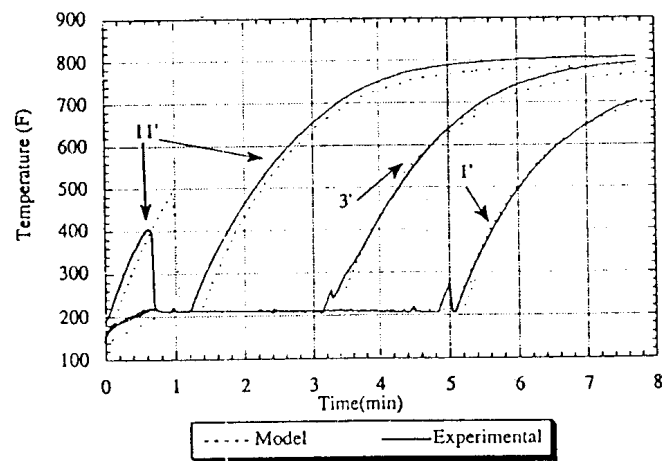


Figure 10. Comparison of calculated and experimental temperature histories for run #3157A

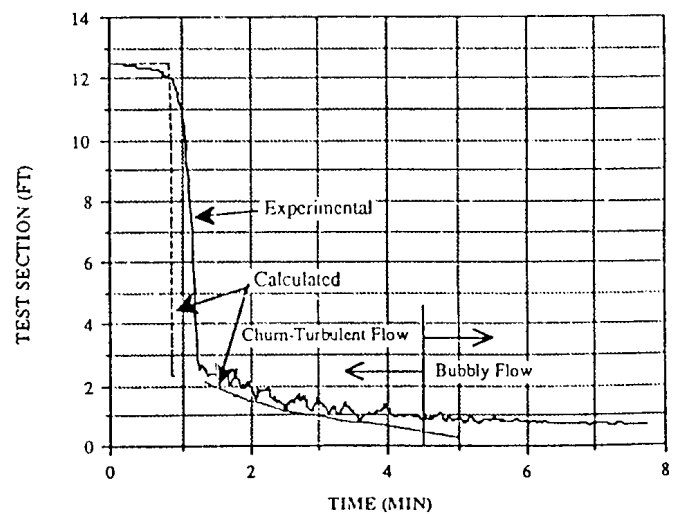


Figure 11. Comparison of calculated and experimental collapsed liquid level history for run #3153B

CONCLUSIONS

In this paper there is studied the dryout of a heated vertical tube, initially containing water. The tests are divided according to the height of the initial liquid column (12, 6.5 or 4 ft), the heat input (6700 to 500 Watts) and the system pressure (1, 2 or 3 atmospheres). For the analysis of the experimental data, each test was divided into three thermal regions of first, second and the third period.

The analysis of the first period formulates the temperature history for that period. It involves a conduction heat transfer solution with an imposed conduction-convection boundary condition.

Next there is presented the analysis and modeling of the second period. There the analysis is based on solving a transient one-dimensional void fraction distribution equation, and then using the solution for solving the collapsed liquid level, two-phase level and the duration of the second period. The problem is simplified by ignoring the instantaneous pressure gradient associated with liquid inertia, ignoring the energy released on the quench front and using drift flux relation for formulating the flow of two phases in the tube.

Finally there is presented the predictions of the dryout, collapsed liquid level and temperature histories of both initially-filled and partially-filled runs during the third period. The models use the method of drift flux velocity and employ the model developed Sun *et al.* for the dryout predictions and the thermal model developed by Yeh *et al.* for the temperature calculations of over the dryout levels. The models of second and the third period are unable to predict the onset of dryout in the tube. Using the experimental data for the first dryout time, the predicted values of the dryout times of lower elevations, the histories of the collapsed liquid levels and the temperature profiles of different levels in the tube are obtained.

The analysis of the three postulated periods are put together in an integrated computer model. The program requires specification of the initial conditions of a test, such as the input power, the initial water temperature and

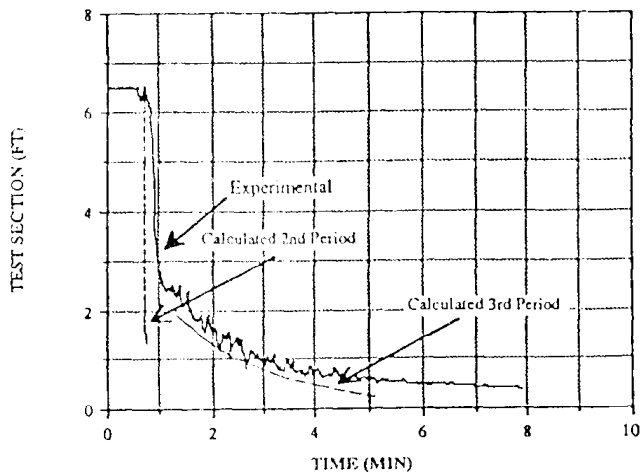


Figure 12. Comparison of calculated and experimental collapsed liquid level history for run #3157A

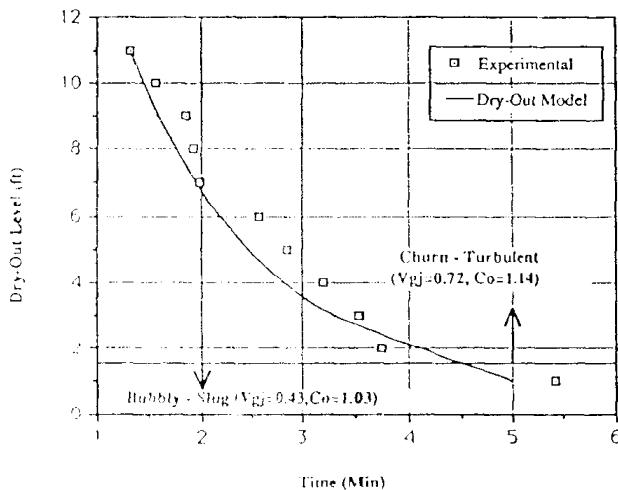


Figure 13. Calculated results v.s. experimental data (run #3153B)

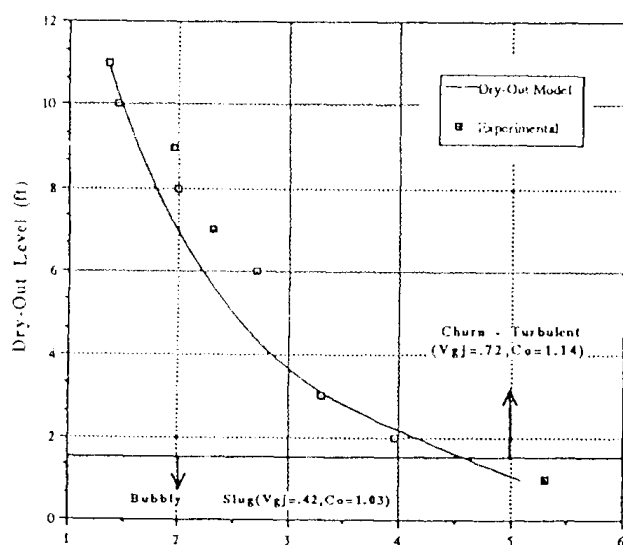


Figure 14. Calculated results v.s. experimental data (run #3157A)

the system pressure for which the test is taken and predicts the temperature, collapsed liquid level and the dryout level histories of the entire test period.

Comparing the results of the numerical model with the experimental results indicates that with the exception of the predicted duration of the second period there is a fair agreement between calculated experimental data for all three periods. The comparisons are in the form of temperature profiles for all three periods, time to reach bulk saturation in the tube, collapsed liquid level for all three periods and dryout history of the third period.

ACKNOWLEDGMENTS

The author wishes to express his sincere gratitude and appreciation to professor R. Seban of the University of California at Berkeley for his contribution to this paper.

NOMENCLATURE

a	Tube inner radius, ft
A_c	Cross sectional area, ft ²
A_T	Total inside tube wall area, ft
B	Parameter $(Q'v_{fg}/A_c h_{fg})$; $B_L = Bv_f/v_g$, 1/sec
C_u	Void distribution parameter
$C_{p,i}$	Specific heat of substance i , Btu/lbm F
D	Tube diameter, ft
g	Gravitational constant, ft/s ²
H	Height, ft
h'_i	Specific enthalpy of phase i , Btu/lbm
h_p	Heat transfer coefficient to the steam, Btu/hr ft ² F
h_L	Heat transfer coefficient to the environment, Btu/hr ft ² F
L	Length, ft
K	Thermal conductivity, Btu/hr ft F
Nu	Nusselt number
M	Mass, lbm
M'	Flow rate, lbm/s
ΔP	Pressure differential, lbm/ft ²
Pr	Prandtl number
P	Power, Btu/hr
Q'	Heat input per unit length of the tube, Btu/hr ft

Q	Input power, Btu/hr
Q_L	Exterior heat loss per unit surface area, Btu/hr-ft ²
q	Heat input rate per cross-sectional area, Btu/hr-ft ²
Re	Reynolds number
t	Time, hr, min, s
U_Q	Quench velocity, ft/s
T	Temperature, F
u_i	Velocity of phase i , ft/s
V	Specific volume, ft ³ /lbm
v_{fg}	$v_g - v_f$, ft ³ /lbm
V_{gj}	Drift flux velocity, ft/s
Z_c	Collapsed liquid level, ft
Z_{10}	Two phase (dry-out) level, ft

Greek Symbols

ρ	Density, lbm/ft ³
$\Delta\rho$	$\rho_l - \rho_g$, lbm/ft ³
α	Void fraction
α_i	Thermal diffusivity of substance i , ft ² /hr
σ	Surface tension, lbf/ft
δ	Thickness of the tube, ft
Γ	Rate of vaporization, lbm/s ft ³
θ	Time difference
μ	Dynamic viscosity

Subscripts

C	Calculated value
D	Dryout
E	Experimental value
f	Liquid
g	Vapor
i	Initial
k	Value of the collapsed liquid level at the end of the second period
L	Heated length of the test tube (12')
o	Quantity at time zero
r	Position of the collapsed liquid level at the beginning of the swelling
sat	Saturated liquid or gas conditions
T	Transition
w	Wall
W	Location of limiting characteristic or continuity wave
∞	Ambient

REFERENCES

1. A. Heydari, "Heat Transfer and Carryover in the Dry-Out of a Heated Vertical Tube," Ph.D. Disserttion, Mechanical Engineering, U. C. Berkeley, (1989).
2. R. A. Zogg, "Pressurized Reflood Systems: Final Design and Operation," ME 299 Project Report, University of California, Berkeley, Ca. (1981).
3. C. A. La Jeunesse, "Investigation of Dry Out Phenomena in a Vertical Tube," ME 299 Project Report, University of California, Berkeley, Ca. (1983).
4. J C. Jaeger, *Proc. Soc. N.S.W.* 74, (1940).
5. H.C. Yeh, J.S. Chiou and M.Y. Young, Heat Transfer Above the Two - Phase Mixture Level Under Core Uncovery Conditions in a 336 - Rod Bundle," *EPRINP*-2161, (1981).
6. R.T. Lahey, Jr., *Nuclear Engineering and Design*, Vol. 45, pp 101-116, (1978).
7. D. W. Condiff and M. Epstein, *Chemical Engineering Science*, Vol. 31, pp. 1139-1148, (1976).
8. N. Zuber, and J. A. Findaly, *Journal of Heat Transfer*, 87C, pp. 453-468, (1965).
9. G. B. Wallis, "One Dimensional Two-Phase Flow," McGraw Hill, (1969).
10. K.H. Sun, R.B. Duffey and C.M. Peng. *Journal of Heat Transfer*, Vol. 103, (1981).
11. R.A. Seban, C.A. La Jeunesse and A. Heydari, "Heat Transfer During Quench and Dryout in a Vertical Tube," *EPRINP*-4157, (1985).